CP-violating ZZh coupling at e^+e^- linear colliders

T. Han* and J. Jiang†
Department of Physics, University of Wisconsin, 1150 University Avenue, Madison, Wisconsin 53706
(Received 27 November 2000; published 6 April 2001)

We study the general Higgs–weak-boson coupling with CP violation via the process $e^+e^- \to f\bar{f}h$. We categorize the signal channels by the subprocesses of Zh production and ZZ fusion and construct four CP asymmetries by exploiting polarized e^+e^- beams. We find complementarity among the subprocesses and the asymmetries to probe the real and imaginary parts of the CP-violating form factor. Certain asymmetries with unpolarized beams can retain significant sensitivity to the coupling. We conclude that at a linear collider with high luminosity, the CP-odd ZZh coupling may be sensitively probed via measurements of the asymmetries.

DOI: 10.1103/PhysRevD.63.096007 PACS number(s): 11.30.Er, 14.80.Cp

I. INTRODUCTION

Searching for a Higgs boson has been a major motivation for many current and future collider experiments, since Higgs bosons encode the underlying physics of mass generation. In the minimal standard model (SM), there is only one CP-even scalar. In the two-Higgs-doublet model or the supersymmetric extension of the SM, there are two CP-even states and one CP-odd state, plus a pair of charged Higgs bosons. The couplings of Higgs bosons to electroweak gauge bosons are particularly important since they faithfully represent the nature of the electroweak gauge symmetry breaking. Determining the detailed properties of the Higgs boson couplings will be of fundamental importance to fully construct the theoretical framework of the electroweak sector.

The most general interaction vertex for a generic Higgs boson (h) and a pair of Z bosons, $Z^\mu(k_1)\ Z^\nu(k_2)\ h$, can be expressed by the following Lorentz structure:

$$\Gamma^{\mu\nu}(k_1,k_2) = i\frac{2}{v}h\,[a\,M_Z^2 g^{\mu\nu} + b\,(k_1^\mu k_2^\nu - k_1\cdot k_2 g^{\mu\nu}) + \tilde{b}\,\epsilon^{\mu\nu\rho\sigma}k_{1\rho}k_{2\sigma}], \tag{1}$$

where $v=(\sqrt{2}G_F)^{-1/2}$ is the vacuum expectation value of the Higgs field, and the Z boson four-momenta are both incoming, as depicted in Fig. 1. The a and b terms are CP even and the $\tilde{b}$ term is CP odd. Thus, the simultaneous existence of terms a (or b) and $\tilde{b}$ would indicate CP violation for the ZZh coupling [1–3]. We note that, in the SM at the tree level, $a=1$ and $b=\tilde{b}=0$. In supersymmetric theories with CP-violating soft supersymmetry (SUSY) breaking terms [4], these CP-violating interactions may be generated by loop diagrams. More generally, the parameters can be momentum-dependent form factors and of complex values to account for the dispersive [Re($\tilde{b}$)] and absorptive [Im($\tilde{b}$)] effects from radiative corrections. Alternatively, in terms of an effective Lagrangian, the b term can be from gauge invariant dimension-6 operators [5], and the $\tilde{b}$ term can be constructed similarly with CP-odd operators involving the dual field tensors. Dimensional analysis implies that the parameters b and $\tilde{b}$ may naturally be of the order of $(v/\Lambda)^2$ where Λ is the scale at which the physics responsible for the electroweak symmetry breaking sets in, presumably $\Lambda \lesssim 4\pi v$. The CP-odd coefficient $\tilde{b}$ is of course very much model dependent.

Possible CP-violation effects via Higgs–gauge-boson couplings have recently drawn a lot of attention in the literature. In Ref. [1], CP-odd observables in decays $h\to ZZ$, W^+W^- and $t\bar{t}$ were constructed. It was discussed extensively how to explore the Higgs properties via the process $e^+e^-\to Zh$ [2,3] at future linear colliders. The polarized photon-photon collisions for $\gamma\gamma\to h$ [6] and the electron-electron scattering process $e^-e^-\to e^-e^-h$ [7] were also considered to extract the CP-violating couplings. There has also been considerable amount of work for investigation of CP-violating Higgs boson interactions with fermions at future e^+e^- colliders [8].

In this paper, we study the CP-violating coupling of ZZh at future e^+e^- linear colliders. In Sec. II, we set out the general consideration, identifying the Zh production and ZZ fusion signals and exploring the generic CP-odd variables by exploiting the polarized beams. Given specific kinematics of the signal processes under investigation, we construct four CP asymmetries in Sec. III. We find important complementarity among the sub-processes and the asymmetries in probing different aspects of the CP-odd coupling, namely the real (dispersive) and imaginary (absorptive) parts of $\tilde{b}$. We also examine to what extent this coupling can be experimentally probed via measurements of the CP asymmetries, with

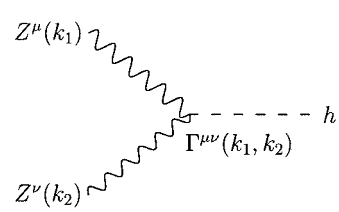

FIG. 1. Vertex function for ZZh coupling.

*Email address: than@egret.physics.wisc.edu
†Email address: jiang@pheno.physics.wisc.edu

and without beam polarization. We present some general discussions of our analyses and summarize our results in Sec. IV.

II. GENERAL CONSIDERATION

We concentrate on the scenario with a light Higgs boson below the *W*-pair threshold. The Higgs–weak-boson coupling will be studied mainly via Higgs boson production, rather than its decay. We focus on the Higgs boson production associated with a fermion pair in the final state

$$e^-(p_1)\, e^+(p_2) \to f(q_1)\, \overline{f}(q_2)\, h(q_3). \tag{2}$$

The Higgs boson signal may be best identified by examining the recoil mass variable

$$m_{rec}^2 = (p_1 + p_2 - q_1 - q_2)^2 = s + m_{ff}^2 - 2\sqrt{s}(E_f + E_{\overline{f}}), \tag{3}$$

where m_{ff} is the $f\overline{f}$ invariant mass and E_f ($E_{\overline{f}}$) is the fermion (anti-fermion) energy in the c.m. frame. This recoil mass variable will yield a peak for the signal at the Higgs boson mass m_h, independent of the Higgs boson decay. This provides a model-independent identification for the Higgs signal. For this purpose, we will accept only

$$f = e^-, \quad \mu^- \quad \text{and} \quad u,\ d,\ s \tag{4}$$

to assure good energy determination for the final state leptons and light quark jets. Whenever appropriate, we adopt energy smearing according to a Gaussian distribution as

$$\frac{\Delta E}{E} = \frac{12\%}{\sqrt{E}} \oplus 1\% \quad \text{for leptons} \tag{5}$$

$$= \frac{45\%}{\sqrt{E}} \oplus 2\% \quad \text{for quarks.} \tag{6}$$

In realistic experimentation, the charged tracking information may also be used to help improve the momentum determination.

As an illustration, the recoil mass spectrum for an e^+e^- final state is shown in Fig. 2 by the dashed curve. The width of the peak in m_{rec} spectrum is determined by the energy resolution of the detector as simulated with Eq. (5). We have also required the final state fermions to be within the detector coverage, assumed to be

$$|\cos\theta_f| < \cos 10° \tag{7}$$

with respect to the beam hole.

A. Zh production versus ZZ fusion

The signal channel Eq. (2) can be approximately divided into two sub-processes

$$e^+e^- \to Zh \quad (Zh \ \text{production}), \tag{8}$$

$$Z^*Z^* \to h \quad (ZZ \ \text{fusion}). \tag{9}$$

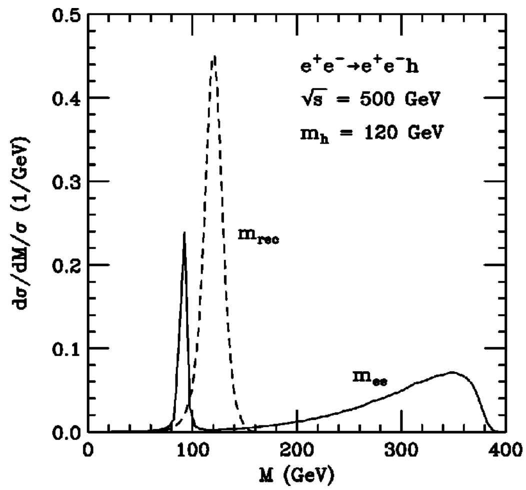

FIG. 2. Normalized mass distributions for $e^+e^- \to e^+e^-h$ at $\sqrt{s}=500$ GeV with $m_h=120$ GeV. The dashed curve is for the recoil mass in Eq. (3), and the solid is for the invariant mass m_{ee}.

Equation (8) yields light fermion states of all flavors from Z decay, while Eq. (9) always has an e^+e^- pair in the final state. These two sub-processes can be effectively distinguished by identifying the final state fermions. Even for the final state of e^+e^-, one can separate them by examining the mass spectrum m_{ee}. This is illustrated in Fig. 2 for the e^+e^- final state by the solid curve. The sharp peak at M_Z indicates the contribution from the decay $Z \to e^+e^-$, while the continuum spectrum at higher mass values is from the ZZ fusion sub-process. In our analysis, we have included both contributions coherently. However, when necessary, we separate out the ZZ fusion contribution by requiring

$$m_{ee} > 100 \ \text{GeV}. \tag{10}$$

The Zh associated production is the leading channel for Higgs boson searches at e^+e^- colliders. ZZ fusion, on the other hand, is often thought to be much smaller due to the small $Z\overline{e}e$ vector coupling and low radiation rate of Z bosons off $e^\pm$ beams. However, the rate of the fusion process increases with c.m. energy logarithmically like $\ln^2(s/M_Z^2)$, and it is also more important for higher Higgs boson masses. The ZZ fusion process naturally leads to a pair of electrons in the final state, which is desirable when the charge information of the final state is needed. Moreover, as a result of the helicity conservation at high energies, the Zh production has only helicity combinations for the initial e^+e^- of $(+-)$ and $(-+)$, while the ZZ fusion has $(--)$ and $(++)$ in addition, where $-(+)$ refers to the left (right) handed helicity. These additional helicity amplitudes may provide further information regarding the CP test, as we will see in the later analysis.

Figure 3 presents the total cross sections for $e^+e^- \to e^+e^-h$ to demonstrate the comparison between the Zh and ZZ fusion processes. Figure 3(a) gives cross sections versus $\sqrt{s}$ for $m_h=110$–200 GeV, and Fig. 3(b) versus m_h for $\sqrt{s} = 350-800$ GeV. The solid curves are for the total SM rate including all contributions coherently, and the dashed curves

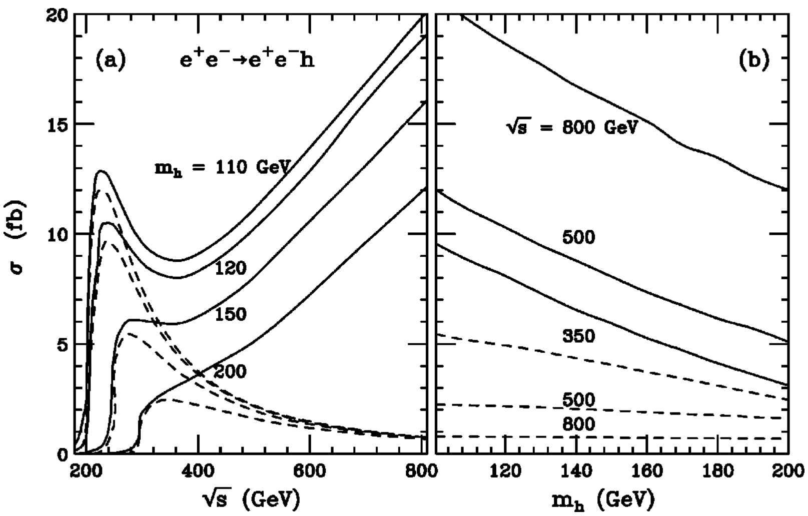

FIG. 3. Total cross sections for $e^+e^-\to e^+e^-h$ in fb (a) versus $\sqrt{s}$ for representative values of m_h, and (b) versus m_h for representative values of $\sqrt{s}$. The dashed curves are for $e^+e^-\to Zh\to e^+e^-h$ only. No kinematical cuts are imposed.

are with a real Z decay for $Zh\to e^+e^-h$. We see that at $\sqrt{s}=500$ GeV and $m_h=120$ GeV, $\sigma(ZZ\to h)\approx 10$ fb$>2\sigma(Zh\to e^+e^-h,\ \mu^+\mu^-h)$. At $\sqrt{s}=800$ GeV and $m_h=120$ GeV, the fusion cross section becomes about an order of magnitude higher than that of $Zh\to e^+e^-h,\ \mu^+\mu^-h$. Clearly, at a linear collider above the Zh threshold, the ZZ fusion process is increasingly more important in studying the Higgs properties [9].

B. *CP* property

To unambiguously identify the effect of CP violation, one needs to construct a ''CP-odd variable,'' whose expectation value vanishes if CP is conserved [10]. We begin our analysis by examining the CP-transformation property. First of all, we note that the initial state of Eq. (2) can be made a CP eigenstate, given the CP-transformation relation

$$e^-(\sigma_1,\vec{p})\, e^+(\sigma_2,-\vec{p})\Rightarrow e^-(-\sigma_2,\vec{p})\, e^+(-\sigma_1,-\vec{p}), \tag{11}$$

where σ_i is the fermion helicity. Now consider a helicity matrix element $\mathcal{M}_{\sigma_1\sigma_2}(\vec{q}_1,\vec{q}_2)$ where σ_1 (σ_2) denotes the helicity of the initial state electron (positron), which coincides with the longitudinal beam polarization; $\vec{q}_1$ ($\vec{q}_2$) denotes the momentum of the final state fermion (antifermion). It is easy to show that, under CP transformation,

$$\mathcal{M}_{-+}(\vec{q}_1,\vec{q}_2)\Rightarrow\mathcal{M}_{-+}(-\vec{q}_2,-\vec{q}_1), \tag{12}$$

$$\mathcal{M}_{--}(\vec{q}_1,\vec{q}_2)\Rightarrow\mathcal{M}_{++}(-\vec{q}_2,-\vec{q}_1), \tag{13}$$

and $\mathcal{M}_{+-}$, $\mathcal{M}_{++}$ transform similarly. If CP is conserved in the reaction, relations (12) and (13) take equal signs. These relations precisely categorize two typical classes of CP test:

CP eigen-process. Under CP, $\mathcal{M}_{-+}$ (or $\mathcal{M}_{+-}$) is invariant if CP is conserved. One can thus construct CP-odd *kinematical variables* to test the CP property of the theory. We can construct a ''forward-backward'' asymmetry

$$\mathcal{A}^{FB}=\sigma^F-\sigma^B=\int_0^1\frac{d\sigma}{d\cos\theta}d\cos\theta-\int_{-1}^0\frac{d\sigma}{d\cos\theta}d\cos\theta, \tag{14}$$

with respect to a CP-odd angular variable θ. This argument is applicable for unpolarized or transversely polarized beams as well.

CP-conjugate process. $\mathcal{M}_{--}$ and $\mathcal{M}_{++}$ are CP conjugate to each other. In this case, instead of a kinematical variable, the appropriate means to examine CP violation is to directly compare the rates of the conjugate processes. We can thus define another CP asymmetry in *total cross section rates* between the two conjugate processes of opposite helicities, called the ''left-right'' asymmetry:

$$\mathcal{A}_{LR}=\sigma_{--}-\sigma_{++}. \tag{15}$$

The longitudinally polarized cross section for arbitrary beam polarizations can be calculated by the helicity amplitudes

$$\begin{aligned}d\sigma(P_-P_+)=\frac{1}{4}[&(1+P_-)(1+P_+)d\sigma_{++}+(1+P_-)\\&\times(1-P_+)d\sigma_{+-}+(1-P_-)(1+P_+)d\sigma_{-+}\\&+(1-P_-)(1-P_+)d\sigma_{--}],\end{aligned} \tag{16}$$

where P_- (P_+) is the electron (positron) longitudinal polarization, with $P_\pm=-1$ $(+1)$ for purely left (right) handed. Whenever appropriate in our later studies, we will assume the realistic beam polarization as $(|P_-|,|P_+|)=(80\%,60\%)$ [11].

III. *CP*-ODD VARIABLES AND THE *CP*-ODD COUPLING

In this section, we construct CP-odd variables for the Higgs signal in Eq. (2) in order to study the CP-violating interactions in Eq. (1). Different CP asymmetries appear to be complementary in exploring different aspects of the CP-odd coupling $\tilde{b}$.

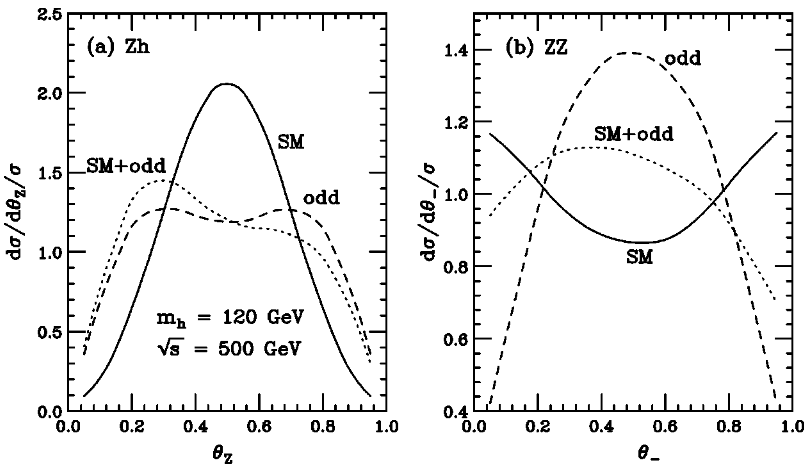

FIG. 4. Normalized polar angle distributions for σ_{-+} at $\sqrt{s}=500$ GeV with $m_h=120$ GeV for (a) $e^+e^-\to Zh$ with $Z\to f\bar{f}$, and (b) $e^+e^-\to e^+e^-h$ via ZZ fusion. The solid curves are for the SM interaction ($a=1$), the dashed for the CP-odd [$\mathrm{Im}(\tilde{b})=1$], and the dotted for CP violation with $a=\mathrm{Im}(\tilde{b})=1$. Here 100% longitudinal polarization of $e_L^- e_R^+$ has been used.

A. Simple polar angles and Im($\tilde{b}$)

It has been argued that the Zh process will test the spin-parity property [2] of the coupling by simply measuring the polar angle distribution of the outgoing Z boson. The distribution can be written in the form

$$\frac{d\sigma}{d\cos\theta_Z}\propto\begin{cases}\beta^2\sin^2\theta_Z+\dfrac{8M_Z^2}{s} & \text{scalar } h,\\ 1-\dfrac{1}{2}\sin^2\theta_Z & \text{pseudo}-\text{scalar } h.\end{cases}$$

In fact, this simple polar angle may provide CP information as well. If we rewrite this angle in terms of a dot product,

$$\cos\theta_Z=\frac{\vec{p}_1\cdot\vec{q}_+}{|\vec{p}_1|\,|\vec{q}_+|},\tag{17}$$

where $\vec{q}_+=\vec{q}_1+\vec{q}_2$ is the vector sum of the outgoing fermion momenta, it is easy to see that it is P odd and C even under transformation for the final state. One could thus expect to test the CP property of the interactions by examining the polar angle distribution. The experimental study is made particularly simple since this variable does not require charge identification for the final state fermions. Because of this, one expects to increase the statistical accuracy by including some well-measured hadronic decay modes of Z, as we accept the light quark jets of Eq. (4). However, after the azimuthal angle integration the dispersive part of the form factor proportional to $\mathrm{Re}(\tilde{b})$ vanishes and the surviving term is the absorptive part proportional to $\mathrm{Im}(\tilde{b})$. The angular distributions are shown in Fig. 4(a) for $\sqrt{s}=500$ GeV with $m_h=120$ GeV. The solid curve is for the SM interaction only ($a=1$), the dashed curve is for the CP-odd only [$\mathrm{Im}(\tilde{b})=1$], and the dotted is for CP violation with $a=\mathrm{Im}(\tilde{b})=1$. We see from the dotted curve that there is indeed an asymmetry with respect to the forward ($\pi/2\leqslant\theta_Z\leqslant 0$) and backward ($\pi\leqslant\theta_Z\leqslant\pi/2$) regions. We have assumed 100% longitudinal polarization of $e_L^- e_R^+$ for illustration here.

The above calculation can in principle be carried through for the ZZ fusion process. However, as a result of the unique kinematics in this process, it appears that we can define an alternative polar angle

$$\cos\theta_-=\frac{(\vec{p}_1\times\vec{q}_-)\cdot(\vec{q}_1\times\vec{q}_2)}{|\vec{p}_1\times\vec{q}_-|\,|\vec{q}_1\times\vec{q}_2|},\tag{18}$$

where $\vec{q}_-=\vec{q}_1-\vec{q}_2$, which yields a larger asymmetry and thus being more sensitive to the coefficient $\mathrm{Im}(\tilde{b})$. It is easy to verify that this variable is P odd and C even under transformation for the final state. Figure 4(b) shows the angular distributions for $e^+e^-\to e^+e^-h$ via ZZ fusion with 100% longitudinal polarization of $e_L^- e_R^+$. The legend is the same as in Fig. 4(a). We see from the dotted curve that an asymmetry exists with respect to this angle.

Replacing θ by θ_Z in Eq. (14), we can define a forward-backward asymmetry $\mathcal{A}_{\theta_Z}^{FB}$ with respect to the angle θ_Z and similarly another asymmetry $\mathcal{A}_{\theta_-}^{FB}$ with respect to the angle θ_-. These two asymmetries are calculated for σ_{-+} and shown in Fig. 5 at $\sqrt{s}=500$ GeV with $m_h=120$ GeV versus $\mathrm{Im}(\tilde{b})$. Figures 5(a) and 5(b) are the asymmetry in fb and the percentage asymmetry respectively, with respect to θ_Z in $Zh\to f\bar{f}h$. Similarly, Figs. 5(c) and 5(d) show the asymmetry and percent asymmetry for ZZ fusion with respect to θ_-. The dashed curves are for 100% longitudinal polarization $e_L^- e_R^+$, the solid are for a realistic polarization $(e_L^-, e_R^+)=(80\%,60\%)$, and the dotted are for unpolarized beams. We see that the beam polarization here substantially enhances the asymmetries, and the realistic polarization maintains the asymmetries to a large extent. Some degree of asymmetry still exists even for unpolarized beams. The percentage asymmetry for the Zh process can be as large as 30% for $\mathrm{Im}(\tilde{b})\sim 0.2$, and is typically of a few percent for ZZ fusion.

We wish to address to what extent an asymmetry can be determined by experiments. For this purpose, we estimate the statistical uncertainties for the asymmetry measurements. We determine the Gaussian statistical error by $\sqrt{N_F+N_B}$

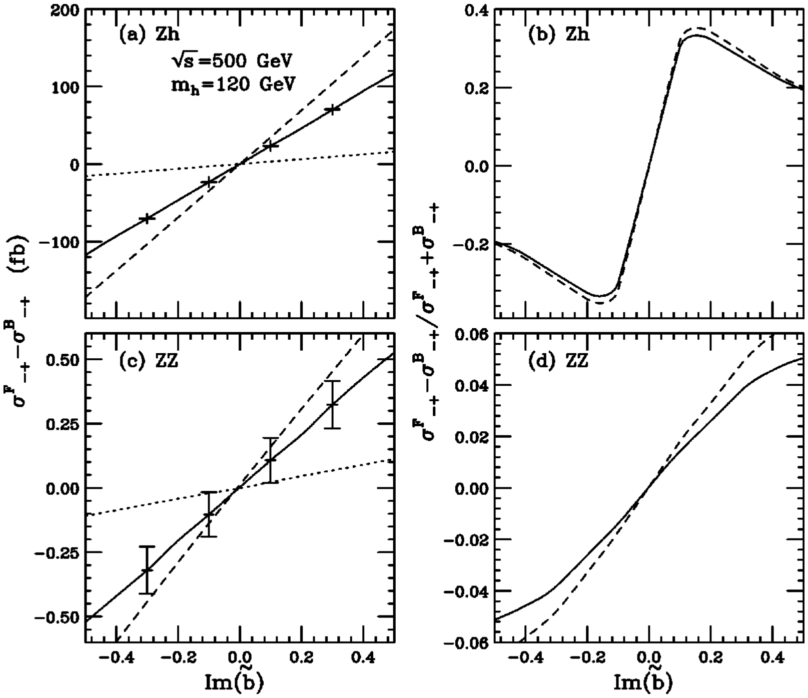

FIG. 5. Forward-backward asymmetries for σ_{-+} versus $\mathrm{Im}(\tilde{b})$ at $\sqrt{s}=500$ GeV with $m_h=120$ GeV for (a) $Zh\to f\bar{f}h$: asymmetry in fb, (b) $Zh\to f\bar{f}h$: percentage asymmetry, (c) ZZ fusion: asymmetry in fb, and (d) ZZ fusion: percentage asymmetry. The dashed curves are for 100% longitudinal polarization $e_L^- e_R^+$, the solid for a realistic polarization $(e_L^-, e_R^+)=(80\%,60\%)$, and the dotted for unpolarized beams. The error bars are statistical uncertainties obtained with a luminosity of 1000 fb^{-1}.

where N_F (N_B) is the number of forward (backward) events. The statistical significance for the asymmetry measurement is obtained by

$$\frac{|N_F-N_B|}{\sqrt{N_F+N_B}}. \tag{19}$$

The error bars in the plots are calculted with an assumed integrated luminosity of 1000 fb^{-1}. Because of the larger asymmetry as well as a larger cross section for $Zh\to f\bar{f}h$, the Zh production would provide a much better determination of $\mathrm{Im}(\tilde{b})$.

As we discussed earlier, the ZZ fusion process can provide another type of asymmetry between CP conjugate processes, in particular between σ_{--} and σ_{++} as defined in Eq. (15), which is absent in Zh production. This is presented in Fig. 6 for $\mathcal{A}_{LR}$, at $\sqrt{s}=500$ GeV with $m_h=120$ GeV versus $\mathrm{Im}(\tilde{b})$. Figure 6(a) is the asymmetry in fb. The legend is the same as in Fig. 5. The error bars are for a total integrated luminosity of 1000 fb^{-1} (500 fb^{-1} each for σ_{--} and σ_{++}). The percentage asymmetry in Fig. 6(b) can be at a 10% level for $\mathrm{Im}(\tilde{b})\sim 0.2$. It is interesting to note that the solid curves yield a non-zero value for $\tilde{b}=0$. This is due to the intrinsic LR asymmetry of the Z coupling to electrons. This shift appears when $|P_-|\neq|P_+|$ and is proportional to $\sigma_{-+}-\sigma_{+-}$. It can be well predicted in the SM for a given beam polarization.

Cross section asymmetries versus $\sqrt{s}$ are shown in Fig. 7 in units of fb with $m_h=120$ GeV (a) forward-backward asymmetry for σ_{-+} in Zh production with respect to θ_Z for $\mathrm{Im}(\tilde{b})=0.1$, (b) forward-backward asymmetry for σ_{-+} in ZZ fusion with respect to θ_- for $\mathrm{Im}(\tilde{b})=0.5$, and (c) LR asymmetry between σ_{--} and σ_{++} for $\mathrm{Im}(\tilde{b})=0.1$. The dashed curves are for 100% longitudinal polarization, and the solid are for a realistic polarization $(e^-,e^+)=(80\%,60\%)$. The error bars are for the statistical uncer-

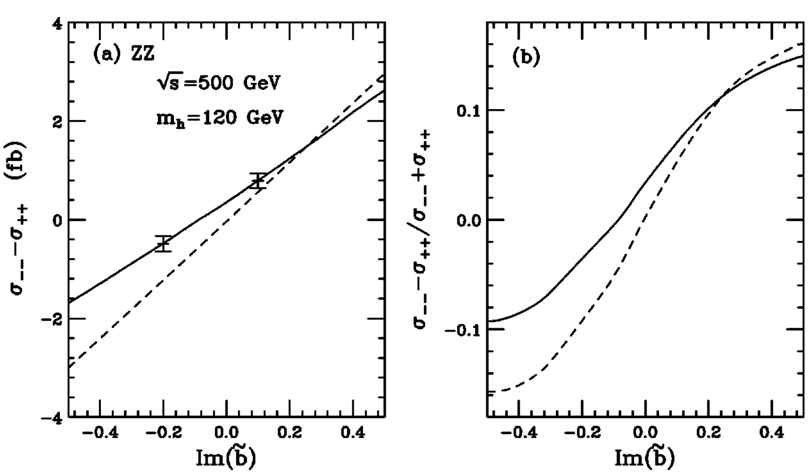

FIG. 6. Polarized cross section asymmetry at $\sqrt{s}=500$ GeV with $m_h=120$ GeV versus $\mathrm{Im}(\tilde{b})$ for (a) the asymmetry in fb, and (b) the percentage asymmetry. The dashed curves are for 100% beam polarization, the solid for a realistic polarization $(e^-,e^+)=(80\%,60\%)$. The error bars are statistical uncertainties obtained with a luminosity of 1000 fb^{-1}.

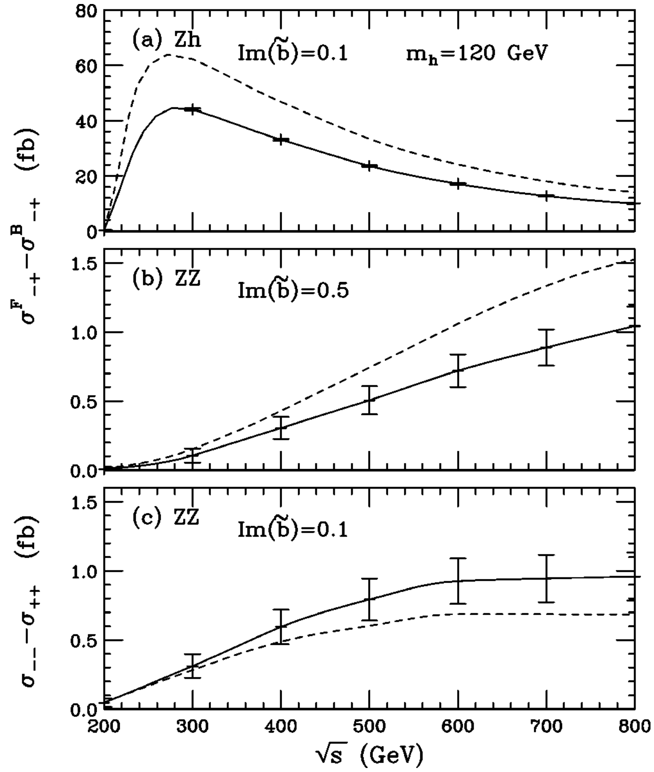

FIG. 7. Cross section asymmetries in fb versus $\sqrt{s}$ with $m_h = 120$ GeV for (a) forward-backward asymmetry with respect to θ_Z for $\mathrm{Im}(\tilde{b}) = 0.1$, (b) forward-backward asymmetry with respect to θ_- for $\mathrm{Im}(\tilde{b}) = 0.5$, (c) LR asymmetry between σ_{--} and σ_{-++} for $\mathrm{Im}(\tilde{b}) = 0.1$. The dashed curves are for 100% longitudinal polarization, and the solid for a realistic polarization $(e^-, e^+) = (80\%, 60\%)$. The error bars are statistical uncertainties obtained with a luminosity of 1000 fb^{-1}.

tainty with a luminosity of 1000 fb^{-1}. We see again the possibly good accuracy for determining the asymmetry by the Zh process. Furthermore, these two processes are complementary: at lower energies near threshold the Zh production is far more important, while at higher energies the ZZ fusion becomes increasingly significant, as has been seen in Fig. 3. In Fig. 7(c), the reason that the realistic asymmetry (solid) is even bigger than the ideal case (dashed) is due to the non-zero contribution from the CP-conserving LR asymmetry of the Z coupling as discussed in the last paragraph.

B. Lepton momentum orientation and Re($\tilde{b}$)

We showed in the last section that the simple polar angles can probe CP violation for a Higgs–gauge-boson coupling, but only for the absorptive part of the form factor $\mathrm{Im}(\tilde{b})$. In order to be sensitive to the dispersive part $\mathrm{Re}(\tilde{b})$, one needs to construct more sophisticated variables, involving the azimuthal angle information for the final state fermions. We find that a simple variable to serve this purpose [12] can be defined as

$$\cos\theta_l = \frac{\vec{p}_1 \cdot (\vec{q}_1 \times \vec{q}_2)}{|\vec{p}_1|\,|\vec{q}_1 \times \vec{q}_2|}, \tag{20}$$

where $\vec{q}_1 \times \vec{q}_2$ defines the orientation of the plane for the final state fermion pair. This variable is P even and C odd under final state transformation. However, we would need to unambiguously identify the fermion from the anti-fermion, and to accurately determine their momenta. This is naturally achievable for the ZZ fusion process, while we will have to limit ourself to $f = e^-, \mu^-$ for the $Zh \to f\bar{f}h$ process. Explicit calculations show that this variable is only sensitive to $\mathrm{Re}(\tilde{b})$ and insensitive to $\mathrm{Im}(\tilde{b})$.

We evaluate the angular distribution for $\cos\theta_l$ at $\sqrt{s} = 500$ GeV with $m_h = 120$ GeV. Shown in Fig. 8 are the normalized distributions for (a) $e^+e^- \to Zh$ with $Z \to e^-e^+, \mu^-\mu^+$ and (b) $e^+e^- \to e^+e^-h$ via ZZ fusion. The solid curves are for the SM interaction ($a = 1$), the dashed curves are for the CP-odd $[\mathrm{Re}(\tilde{b}) = 1]$, and the dotted are for CP violation with $a = \mathrm{Re}(\tilde{b}) = 1$. Here 100% longitudinal polarization of $e_L^- e_R^+$ has been used as for σ_{-+}. The CP asymmetries are manifest as seen from the dotted curves. We define a CP asymmetry $\mathcal{A}_{\theta_l}^{FB}$ in the same way as in Eq. (14). The asymmetries for these two processes are calculated for σ_{-+}, and shown in Fig. 9 at $\sqrt{s} = 500$ GeV with $m_h = 120$ GeV versus $\mathrm{Re}(\tilde{b})$. The parameters and legend are the same

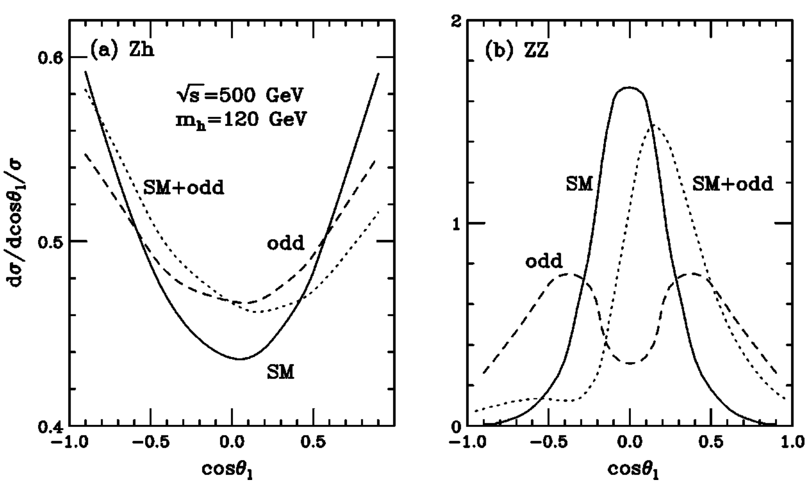

FIG. 8. Normalized angular distributions for σ_{-+} at $\sqrt{s} = 500$ GeV with $m_h = 120$ GeV for (a) $e^+e^- \to Zh$ with $Z \to e^-e^+, \mu^-\mu^+$ and (b) $e^+e^- \to e^+e^-h$ via ZZ fusion. The solid curves are for the SM interaction ($a = 1$), the dashed for the CP-odd $[\mathrm{Re}(\tilde{b}) = 1]$, and the dotted for CP violation with $a = \mathrm{Re}(\tilde{b}) = 1$. Here 100% longitudinal polarization of $e_L^- e_R^+$ has been used.

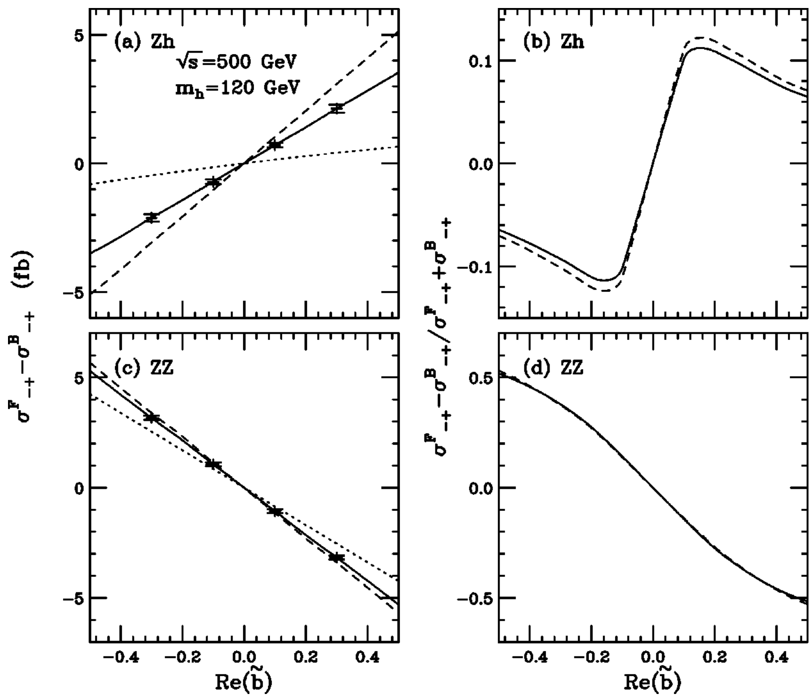

FIG. 9. Forward-backward asymmetry for σ_{-+} versus $\mathrm{Re}(\tilde{b})$ at $\sqrt{s}=500$ GeV with $m_h=120$ GeV for (a) $Zh \to f\bar{f}h$: asymmetry in fb, (b) $Zh \to f\bar{f}h$: percentage asymmetry, (c) ZZ fusion: asymmetry in fb, and (d) ZZ fusion: percentage asymmetry. The dashed curves are for 100% longitudinal polarization $e_L^- e_R^+$, the solid for a realistic polarization $(e_L^-, e_R^+)=(80\%,60\%)$, and the dotted for unpolarized beams. The error bars are statistical uncertainties obtained with a luminosity of 1000 fb^{-1}.

as in Fig. 5. We see that the percentage asymmetry for the Zh process is about 10% percent and for ZZ fusion it can be as large as 30% for $\mathrm{Re}(\tilde{b}) \approx 0.2$. The error bars in the plots are estimated with an integrated luminosity of 1000 fb^{-1}. As a result of the large asymmetries, both Zh production and ZZ fusion processes could provide a good probe to the coupling $\mathrm{Re}(\tilde{b})$. A particularly important result as indicated in Figs. 9(c) and 9(d) is that the asymmetry for the ZZ fusion is rather insensitive to the beam polarization.

Forward-backward cross section asymmetries for σ_{-+} with respect to θ_l are shown versus $\sqrt{s}$ in Fig. 10 with $m_h=120$ GeV and $\mathrm{Re}(\tilde{b})=0.1$. Figure 10(a) is the asymmetry for Zh production, and Fig. 10(b) is for ZZ fusion. We see again good sensitivity for measuring the asymmetry especially by the ZZ fusion process and at higher energies, which appears to have very little dependence on the beam polarization.

To further assess the linear collider sensitivity to $\tilde{b}$, we compare all the CP asymmetries and present in Table I the 95% confidence level (2σ) sensitivity limits with $m_h=120$ GeV for two collider energies $\sqrt{s}=500$, 800 GeV and two choices of integrated luminosity $\mathcal{L}=500$, 1000 fb^{-1}. Realistic polarizations of (80%, 60%) are used unless specified for no beam polarization by ''unpolarized.'' We see that at a 500 GeV linear collider with a total luminosity of 1000 fb^{-1}, the CP-odd coupling form factor may be sensitively probed to a value of about $\mathrm{Im}(\tilde{b}) \approx 0.0022$ and $\mathrm{Re}(\tilde{b}) \approx 0.017$ at a 95% C.L. The coupling may even be probed without a beam polarization to a level of about $\mathrm{Im}(\tilde{b}) \approx 0.013$ and $\mathrm{Re}(\tilde{b}) \approx 0.018$. The beam polarization improves the sensitivity to $\mathrm{Im}(\tilde{b})$ by about a factor of 5–6 via $\mathcal{A}^{FB}_{\theta_Z}(Zh)$, but does little to $\mathrm{Re}(\tilde{b})$ through $\mathcal{A}^{FB}_{\theta_l}(ZZ)$. At $\sqrt{s}=800$ GeV, the sensitivity in Zh process is slightly degraded. On the other hand, the sensitivity in ZZ fusion is enhanced by about a factor of 2 due to the larger cross section and larger asymmetry at higher energies.

IV. DISCUSSIONS AND CONCLUSIONS

Before summarizing our results, a few remarks are in order. First, in previous studies of the Zh process [2,3], a common variable is defined as

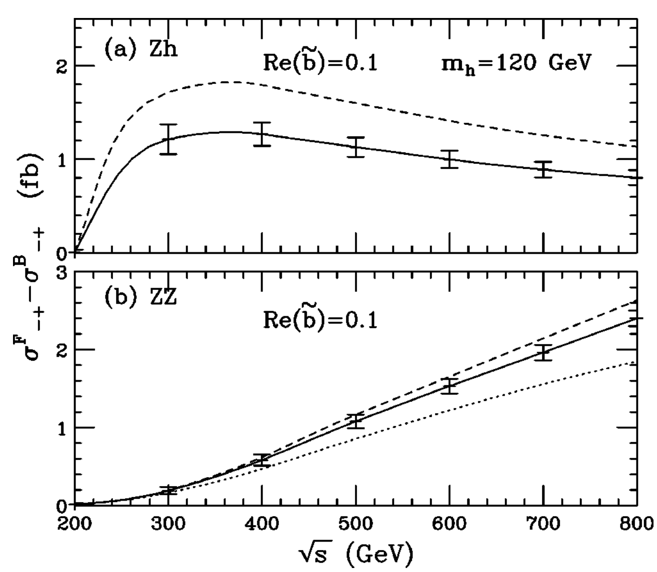

FIG. 10. Forward-backward cross section asymmetries for σ_{-+} with respect to θ_l in fb versus $\sqrt{s}$ with $m_h=120$ GeV and $\mathrm{Re}(\tilde{b})=0.1$ for (a) Zh production and (b) ZZ fusion. The dashed curves are for 100% longitudinal polarization and the solid for a realistic polarization $(e^-,e^+)=(80\%,60\%)$. The error bars are statistical uncertainties obtained with a luminosity of 1000 fb^{-1}.

TABLE I. 95% C.L. limits on $\tilde{b}$ from the CP asymmetries defined in the text at $\sqrt{s}=500$, 800 GeV with $m_h=120$ GeV, for two representative luminosities $\mathcal{L}=500$, 1000 fb^{-1}. Realistic polarizations of (80%, 60%) are used unless specified as ''unpolarized.''

	$\sqrt{s}$ (GeV)	500	500	800	800
	$\mathcal{L}$(fb^{-1})	500	1000	500	1000
Im($\tilde{b}$)	$\mathcal{A}^{FB}_{\theta_Z}(Zh)$ [$-+$]	0.0028	0.0022	0.0043	0.0032
	$\mathcal{A}^{FB}_{\theta_Z}(Zh)$ [unpol.]	0.019	0.013	0.025	0.019
	$\mathcal{A}^{FB}_{\theta_-}(ZZ)$ [$-+$]	0.21	0.16	0.19	0.13
	$\mathcal{A}_{LR}(ZZ)$	0.071	0.045	0.065	0.041
Re($\tilde{b}$)	$\mathcal{A}^{FB}_{\theta_l}(Zh)$ [$-+$]	0.023	0.018	0.019	0.014
	$\mathcal{A}^{FB}_{\theta_l}(ZZ)$ [$-+$]	0.021	0.017	0.014	0.009
	$\mathcal{A}^{FB}_{\theta_l}(ZZ)$ [unpol.]	0.024	0.018	0.016	0.010

$$\cos\theta_+ = \frac{(\vec{p}_1\times\vec{q}_+)\cdot(\vec{q}_1\times\vec{q}_2)}{|\vec{p}_1\times\vec{q}_+|\,|\vec{q}_1\times\vec{q}_2|}, \tag{21}$$

where $\vec{q}_+=\vec{q}_1+\vec{q}_2=\vec{p}_Z$. This variable seems quite suitable for the Zh production since it is the azimuthal angle formed between the Zh production plane and the decay plane of $Z\to f\bar{f}$ if the Z momentum is chosen to define the rotational axis. However, this variable is P even and C even under final state transformation and thus cannot provide an unambiguous measure for CP violation alone. One would have to analyze other angular distributions to extract the CP property of the interaction.

As a second remark, one may consider our analysis for the ZZ fusion similar to that in e^-e^- collisions [7], since the only tree-level Higgs boson production at e^-e^- colliders is via the ZZ fusion mechanism [13]. However, an e^-e^- initial state cannot be made a CP eigenstate as evident from the discussion of Eq. (11). The explicit CP asymmetry in e^-e^- collisions would have to be constructed in comparison with the conjugate e^+e^+ reactions.

Finally, although the ZZh coupling under current investigation is arguably the most important interaction in the light of electroweak symmetry breaking, other interaction vertices such as $Z\gamma h$ and $\gamma\gamma h$ may be equally possible to contain CP violation induced by loop effects. Although the CP asymmetries constructed in this paper should be generically applicable to the other cases as well, we choose not to include those coupling in our analyses for the sake of simplicity. However, in terms of our ZZ fusion study, since the photon-induced processes $\gamma\gamma\to h, \gamma Z\to h$ would mainly give collinear electrons along the beams, our kinematical requirement to tag e^+e^- final state at a large angle will effectively single out the ZZh contribution.

To summarize our analyses of possible CP violation for the interaction vertex ZZh, we classified the signal channel into two categories as Zh production with $Z\to f\bar{f}$ and ZZ fusion. We proposed four simple CP-asymmetric variables

$$\mathcal{A}^{FB}_{\theta_Z}: \quad \text{for } Zh \text{ production,}$$

$$\mathcal{A}^{FB}_{\theta_-}: \quad \text{for } ZZ \text{ fusion,}$$

$$\mathcal{A}_{LR}: \quad \text{for } ZZ \text{ fusion only,}$$

$$\mathcal{A}^{FB}_{\theta_l}: \quad \text{for both } Zh,\ ZZ.$$

We found them complementary in probing the CP-odd coupling form factor $\tilde{b}$. The first three are sensitive to Im($\tilde{b}$), while the last one sensitive to Re($\tilde{b}$). Here $\mathcal{A}^{FB}_{\theta_Z}$ yields the largest asymmetry for Im($\tilde{b}$) (see Fig. 5), while $\mathcal{A}^{FB}_{\theta_l}$ is the largest for Re($\tilde{b}$) (see Fig. 9), both reaching about 30% for $|\tilde{b}|\approx 0.2$. The ultimate sensitivity to $\tilde{b}$ depends on both the size of asymmetry and the signal production rate. As illustrated in Table I, at a 500 GeV linear collider with a total luminosity of 1000 fb^{-1}, the CP-odd coupling may be sensitively probed to a value of about Im($\tilde{b}$)$\approx$0.0022 and Re($\tilde{b}$)$\approx$0.017 at a 95% C.L. with the beam polarization (80%, 60%). The coupling may even be probed without beam polarization to a level of about Im($\tilde{b}$)$\approx$0.013 and Re($\tilde{b}$)$\approx$0.018. At a higher energy collider with $\sqrt{s}=800$ GeV, the sensitivity in Zh process is slightly degraded but that in ZZ fusion is enhanced by about a factor of 2.

ACKNOWLEDGMENTS

We thank R. Sobey for his early participation in this project. We would also like to thank K. Hagiwara, W.-Y. Keung, G. Valencia and P. Zerwas for helpful discussions. This work was supported in part by a DOE grant No. DE-FG02-95ER40896 and in part by the Wisconsin Alumni Research Foundation.

[1] D. Chang, W.-Y. Keung, and I. Phillips, Phys. Rev. D **48**, 3225 (1993); A. Soni and R.M. Xu, *ibid.* **48**, 5259 (1993); A. Skjold and P. Osland, Phys. Lett. B **329**, 305 (1994).

[2] V. Barger, K. Cheung, A. Djouadi, B.A. Kniehl, and P.M. Zerwas, Phys. Rev. D **49**, 79 (1994); M. Kramer, J. Kuhn, M.L. Stong, and P.M. Zerwas, Z. Phys. C **64**, 21 (1994).

[3] K. Hagiwara and M. Stong, Z. Phys. C **62**, 99 (1994); J.P. Ma and B.H.J. McKellar, Phys. Rev. D **52**, 22 (1995); A. Skjold and P. Osland, Nucl. Phys. **B453**, 3 (1995); W. Kilian, M. Kramer, and P.M. Zerwas, Phys. Lett. B **381**, 243 (1996); D.A. Demir, Phys. Rev. D **60**, 055006 (1999); Phys. Lett. B **465**, 177 (1999); K. Hagiwara, S. Ishihara, J. Kamoshita, and B.A. Kniehl, Eur. Phys. J. C **14**, 457 (2000).

[4] A. Pilaftsis, Phys. Lett. B **435**, 88 (1998); Phys. Rev. D **58**, 096010 (1998); A. Pilaftsis and C.E.M. Wagner, Nucl. Phys. **B553**, 3 (1999); D. A. Demir, Phys. Rev. D **60**, 055006 (1999); S.Y. Choi, M. Drees, and J.-S. Lee, Phys. Lett. B **481**, 57 (2000).

[5] K. Hagiwara, S. Ishhara, R. Szalapski, and D. Zeppenfeld, Phys. Rev. D **48**, 2182 (1993).

[6] B. Grzadkowski and J.F. Gunion, Phys. Lett. B **294**, 361 (1992); S.Y. Choi, K. Hagiwara, and M.S. Baek, Phys. Rev. D **54**, 6703 (1996); G.J. Gounaris and G.P. Tsirigoti, *ibid.* **56**, 3030 (1997); **58**, 059901(E) (1998).

[7] C.A. Boe, O.M. Ogreid, P. Osland, and J.-Z. Zhang, Eur. Phys. J. C **9**, 413 (1999).

[8] A. Ilakovac, B. A. Kniehl, and A. Pilaftsis, Phys. Lett. B **317**, 609 (1993); X.-G. He, J.P. Ma, and B. McKellar, Phys. Rev. D **49**, 4548 (1994); A. Pilaftsis and M. Nowakowski, Int. J. Mod. Phys. A **9**, 1097 (1994); B. Grzadkowski and J.F. Gunion, Phys. Lett. B **350**, 218 (1995); J.F. Gunion, B. Grzadkowski, and X.-G. He, Phys. Rev. Lett. **77**, 5172 (1996); S. Bar-Shalom, D. Atwood, G. Eilam, R.R. Mendel, and A. Soni, Phys. Rev. D **53**, 1162 (1996); S. Bar-Shalom, D. Atwood, and A. Soni, Phys. Lett. B **419**, 340 (1998); K.S. Babu, C. Kolda, J. March-Russell, and F. Wilczek, Phys. Rev. D **59**, 016004 (1999); B. Grzadkowski, J.F. Gunion, and J. Kalinowski, *ibid.* **60**, 075011 (1999); Phys. Lett. B **480**, 287 (2000); B. Grzadkowski and J. Pliszka, Phys. Rev. D **60**, 115018 (1999); E. Asakawa, S.Y. Choi, K. Hagiwara, and J.S. Lee, *ibid.* **62**, 115005 (2000).

[9] J.F. Gunion, T. Han, and R. Sobey, Phys. Lett. B **429**, 79 (1998).

[10] G. Valencia, in *CP Violation and the Limits of the Standard Model*, Proceedings of the Theoretical Advanced Study Institute, Boulder, Colorado, 1994, edited by J. Donoghue (World Scientific, Singapore, 1995), hep-ph/9411441.

[11] P. Zerwas, plenary talk presented at The 5th International Linear Collider Workshop, Fermilab, 2000.

[12] The same variable has been used for different processes; see, e.g., A.A. Likhoded, G. Valencia, and O.P. Yushchenko, Phys. Rev. D **57**, 2974 (1998).

[13] V. Barger, J. Beacom, K. Cheung, and T. Han, Phys. Rev. D **50**, 6704 (1994); T. Han, Int. J. Mod. Phys. A **11**, 1541 (1996).